Communication

Controlling Molecular Diffusion in Self-Spreading Lipid Bilayer Using Periodic Array of Ultra-Small Metallic Architecture on Solid Surface

Hideki Nabika, Atsushi Sasaki, Baku Takimoto, Yoshitaka Sawai, Shengtai He, and Kei Murakoshi

J. Am. Chem. Soc., **2005**, 127 (48), 16786-16787• DOI: 10.1021/ja0559597 • Publication Date (Web): 11 November 2005

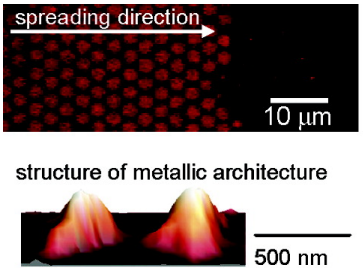

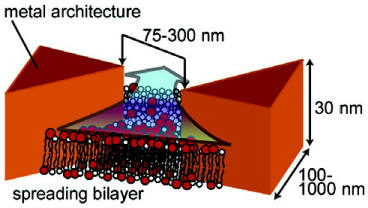

More About This Article

Additional resources and features associated with this article are available within the HTML version:

- Supporting Information
- Links to the 9 articles that cite this article, as of the time of this article download
- Access to high resolution figures
- Links to articles and content related to this article
- Copyright permission to reproduce figures and/or text from this article

View the Full Text HTML

J|A|C|S
COMMUNICATIONS

Published on Web 11/11/2005

Controlling Molecular Diffusion in Self-Spreading Lipid Bilayer Using Periodic Array of Ultra-Small Metallic Architecture on Solid Surface

Hideki Nabika,[†] Atsushi Sasaki,[†] Baku Takimoto,[†] Yoshitaka Sawai,[†] Shengtai He,[‡] and Kei Murakoshi*[,†,‡]

Department of Chemistry, Graduate School of Science, Hokkaido University, Sapporo, 060-0810, Japan, and PRESTO, Japan Science and Technology Agency, Sapporo, 060-0810, Japan

Received August 30, 2005; E-mail: kei@sci.hokudai.ac.jp

Control of molecular motion in confined space is recognized as one of the most important subjects for further developments in advanced ultra-small devices. Recent activities focusing on the application of a two-dimensional small array yielded rectified molecular motions in Brownian ratchet[1] or entropic trap,[2] which are capable of sorting, separating, purifying, and fractionating various large molecules such as DNA.[3] Further precise tuning of the selectivity on molecular characteristics can be achieved if one can clarify the roles working on the situation where target molecules are confined in the space less than a few hundreds nanometers. In this communication, we demonstrate that control of the diffusion of target molecules in the self-spreading lipid bilayer can be achieved when the size of a gap between small metal architectures was changed to be less than a few hundred nanometers. Lipid bilayer was used as a sieving medium here,[1a,3h] because the self-spreading nature of bilayer offers net directional flow for the embedded molecules of interest without any bias from the outside.[4] The self-spreading dynamics of the lipid bilayer depending on the size of the small gap were analyzed to explain the retardation of the target molecules incorporated in the spreading bilayer.

Lipid bilayer, L-α-phosphatidylcholine from egg yolk (egg-PC), mixed with 1 mol % TR-DHPE showed the self-spreading behavior on a Si substrate covered with thin oxide layer (d < 1 nm) in 100 mM NaCl aqueous solution. The spreading dynamics changed depending on the size of periodic array of gold nanoarchitecture fabricated by the nanosphere lithography (NSL)[5] on the surface of a Si substrate. The substrates with the architectures prepared by the polystyrene beads with different diameters, 3000, 1000, 750, and 350 nm, are denoted as NSL3000, NSL1000, NSL750, and NSL350, respectively (Figure 1A). Estimated sizes of the gap between the metal nanoarchitectures on NSL3000, NSL1000, NSL750, and NSL350, were 300, 150, 100, and 75 nm, respectively. Spreading behavior of a single bilayer was monitored in situ by a fluorescence microscope. Typical fluorescence image of spreading bilayer on NSL3000 is shown in Figure 1B. It has been proved experimentally that the diffusion of lipid molecules on gold surface is efficiently prevented because of its surface hydrophobicity.[6] Thus, the dark part in Figure 1B may correspond to the gold architectures which were not covered by the bilayer. It is reasonable to assume that the bilayer spreads through the small gap between the gold architectures.

Figure 2A shows the spreading distance of the bilayer on various substrates as a function of time. It was shown that the spreading distance became smaller as the size of the architectures decreased. For more quantitative discussion on the spreading dynamics, time-dependent change in the velocity of the spreading was analyzed by a double-logarithmic plot of spreading velocity to the spreading time (Figure 2B). All of the plots obtained at different substrates show linearity with the slope of −0.5. It has been shown that the

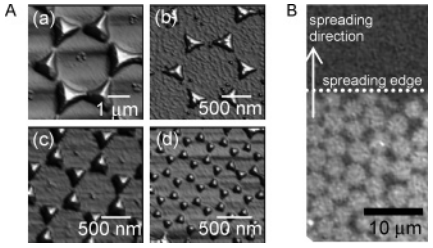

Figure 1. (A) AFM images of (a) NSL3000, (b) NSL1000, (c) NSL750, and (d) NSL350 substrates. (B) Fluorescence image of a spreading lipid bilayer on NSL3000.

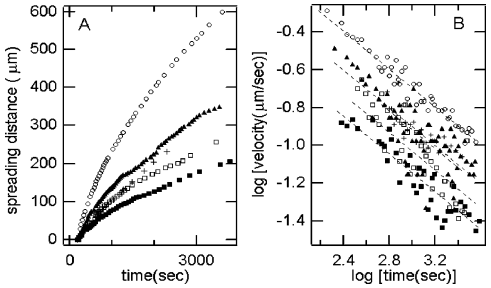

Figure 2. (A) Spreading distance and (B) spreading velocity of self-spreading lipid bilayer as a function of time on bare Si (○), NSL3000 (▲), NSL1000 (×), NSL750 (□), and NSL350 (■). Broken lines in (B) represent the result from a least-squares fit to eq 2.

driving force of the self-spreading can be considered as the gain in free energy per unit area, S, which is dissipated by a friction,[4a,b]

$$S = \gamma_h L(t) v(t) \tag{1}$$

where γ_h is a drag coefficient, $L(t)$ is spreading distance, and $v(t)$ is spreading velocity. The integration of eq 1 gives

$$\log v(t) = \frac{1}{2}\log \beta - \frac{1}{2}\log t \tag{2}$$

where $\beta = S/2\gamma_h$ is referred to as the spreading coefficient. These relations explain the linear relation in the double logarithmic plot with the slope of −0.5. The values of experimentally obtained β from the fitting to Figure 2B and previously documented γ_h (= 10^6 Ns/m^3)[4b] give $S_{Si} = 80 \times 10^{-6}$ J/m^2, which agrees well with the reported value ($\sim 100 \times 10^{-6}$ J/m^2).[4a,b]

In the present system, β deceased significantly as the size of the architectures decreased. Introduction of the architecture may alter the value of S rather than that of γ, because the effect of lateral shear stress to decrease γ is expected to be negligible.[4b] Thus, the spreading coefficient β can be rewritten as

$$\beta_{metal} = \frac{S_{Si} - E_{metal}}{2\gamma_h} \tag{3}$$

[†] Hokkaido University.
[‡] Japan Science and Technology Agency.

10.1021/ja0559597 CCC: $30.25

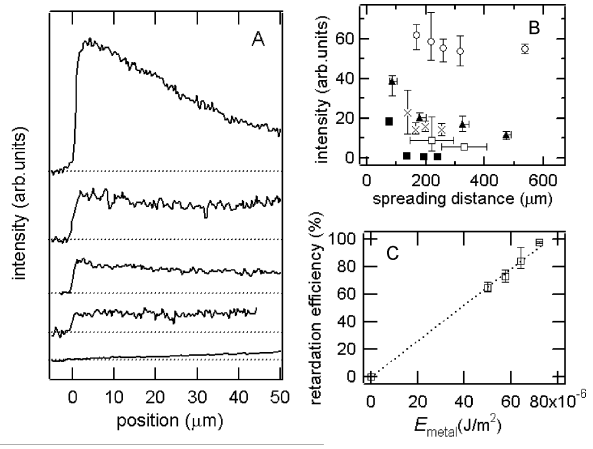

Figure 3. (A) Fluorescence intensity profiles on Si, NSL3000, NSL1000, NSL750, and NSL350 substrates (from upper to lower) after spreading for 10 min. (B) Fluorescence intensity at the spreading edge as a function of the spreading distance on bare Si (○), NSL3000 (▲), NSL1000 (×), NSL750 (□), and NSL350 (■). (C) Relationship between the retardation efficiency (at 200 μm) and E_{metal}. The dotted line is a guide for the eyes.

where E_{metal} is the energy dissipation caused by the presence of the architectures. Fitting the data using eqs 2 and 3 yielded E_{metal} values of 50.0, 57.4, 64.0, and 72.0 μJ/m^2 for NSL3000, 1000, 750, and 350, respectively. These quantitative estimations show that the spreading of bilayer through the small gaps in the size range less than a few hundreds nanometers results in the dissipation of more than half of the intrinsic driving force.

The presence of the metal architecture exhibited not only the change in the spreading velocity, but also an intriguing effect on a molecular distribution profile within the spreading bilayer. Figure 3A displays fluorescence intensity profiles as the function of the distance from the spreading edge. On the Si substrate without the metal architecture, the intensity profile of the doped fluorescent molecules, TR-DHPE, in the spreading bilayer exhibited typical pseudo-exponential decay from the spreading edge (position = 0) into the interior of the bilayer.[4b] However, these exponential decay characteristics disappeared by the introduction of the architecture. Distribution of the molecules decreased as the size of the architecture became small. On NSL350 with the smallest size of the architecture, almost no fluorescence signal was observed at the spreading edge. The fluorescence intensity at the spreading edge became weaker as the spreading proceeded (Figure 3B). Weaker fluorescence at the substrate with a smaller size of the architecture was a general tendency during the entire spreading. The present observation proves that the progress of TR-DHPE molecules is selectively retarded in the spreading bilayer on the substrates with the metal architecture.

To clarify the correlation between the energy dissipation of the spreading bilayer and the retardation of the doped molecule, the retardation efficiency, R, which was defined as $(I_{Si} - I_{NSL})/I_{Si} \times 100$, where I_{Si} and I_{NSL} are the fluorescence intensities at the spreading edge after spreading over a given distance (200 μm), was plotted as the function of E_{metal} (Figure 3C). The plot shows that values of R have a linear correlation with E_{metal}. This linear correlation implies that the retardation can be tuned by changing the size of the gap with the architecture, giving appropriate E_{metal}. Taking into account an elastic nature of lipid bilayer,[7] local compression would be imposed on the spreading bilayer, which is passing through the ultra-small gap. Highly localized compression distorts a bilayer structure significantly, leading to relatively high E_{metal}. Local compression of the spreading bilayer increases a density of egg-PC molecules at the gap region. This imposes an energetic disadvantage for balky TR-DHPE molecules to pass through the gap, leading to the segregation of TR-DHPE from the front edge of the spreading bilayer. Disappearance of TR-DHPE molecules at the edge on NSL350 demonstrates that the compression of the spreading bilayer at the gap less than a few hundred nanometers can achieve complete separation of TR-DHPE molecules from the spreading bilayer.

The present molecular separation originates from a locally enhanced chemical potential barrier induced by the compression of the bilayer membrane. The fact indicates that an intermolecular interaction is a key factor to determine the separation efficiency and selectivity. Thus, the present system can be extended to various kinds of controlled interactions, such as steric hindrance, electrostatic interaction, or stereoselective chiral interaction, etc. These characteristics of the system could lead to a novel molecular separation system showing extremely high selectivity with low-energy consumption. Further tuning of the geometrical structure of the architecture will enable us to sort, separate, and manipulate molecules within the self-spreading bilayer by extremely low input energy.

Supporting Information Available: Procedure for preparing NSL substrate. This material is available free of charge via the Internet at http://pubs.acs.org.

References

(1) (a) van Oudenaarden, A.; Boxer, S. G. *Science* **1999**, *285*, 1046. (b) Bader, J. S.; Deem, M. W.; Hammond, R. W.; Henck, S. A.; Simpson, J. W.; Rothberg, J. M. *Appl. Phys. A* **2002**, *75*, 275. (c) Bader, J. S.; Hammond, R. W.; Henck, S. A.; Deem, M. W.; McDermott, G. A.; Bustillo, J. M.; Simpson, J. W.; Mulhern, G. T.; Rothberg, J. M. *Proc. Natl. Acad. Sci. U.S.A.* **1999**, *96*, 13165. (d) Huang, L. R.; Silberzan, P.; Tegenfeldt, J. O.; Cox, E. C.; Sturm, J. C.; Austin, R. H.; Craighead, H. *Phys. Rev. Lett.* **2002**, *89*, 178301. (e) Cabodi, M.; Chen, Y.; Turner, S. W. P.; Craighead, H. G.; Austin, R. H. *Electrophoresis* **2002**, *23*, 3496. (f) Chou, S.; Bakajin, O.; Turner, S. W. P.; Duke, T. A. J.; Chan, S. S.; Cox, E. C.; Craighead, H. G.; Austin, R. H. *Proc. Natl. Acad. Sci. U.S.A.* **1999**, *96*, 13762. (g) Huang, L. R.; Cox, E. C.; Austin, R. H.; Strum, J. C. *Anal. Chem*. **2003**, *75*, 6963.

(2) (a) Bakajin, O.; Duke, T. A. J.; Tegenfeldt, J.; Chou, C. F.; Chan, S. S.; Austin, R. H.; Cox, E. C. *Anal. Chem*. **2001**, *73*, 6053. (b) Streek, M.; Schmid, F.; Duong, T. T.; Ros, A. *J. Biotechnol.* **2004**, *112*, 79. (c) Han, J.; Craighead, H. G. *J. Vac. Sci. Technol., A* **1999**, *17*, 2142. (d) Han, J.; Craighead, H. G. *Science* **2000**, *288*, 1026. (e) Nykypanchuk, D.; Strey, H. H.; Hoagland, D. A. *Science* **2002**, *297*, 987. (f) Inatomi, K.; Izuo, S.; Lee, S.; Ohji, H.; Shiono, S. *Microelectron. Eng.* **2003**, *70*, 13. (g) Tessier, F.; Labrie, J.; Slater, G. W. *Macromolecules* **2002**, *35*, 4791.

(3) (a) Huang, L. R.; Tegenfeldt, J. O.; Kraeft, J. J.; Strum, J. C.; Austin, R. H.; Cox, E. C. *Nat. Biotechnol*. **2002**, *20*, 1048. (b) Kaji, N.; Tezuka, Y.; Takamura, Y.; Ueda, M.; Nishimoto, T.; Nakanishi, H.; Horiike, Y.; Baba, Y. *Anal. Chem.* **2004**, *76*, 15. (c) Turner, S. W.; Perez, A. M.; Lopez, A.; Craighead, H. G. *J. Vac. Sci. Technol., B* **1998**, *16*, 3835. (d) Seo, Y. S.; Luo, H.; Samuilov, V. A.; Rafailovich, M. H.; Sokolov, J.; Gersappe, D.; Chu, B. *Nano Lett.* **2004**, *4*, 659. (e) Chou, H. P.; Spence, C.; Scherer, A.; Quake, S. *Proc. Natl. Acad. Sci. U.S.A.* **1999**, *96*, 11. (f) Volkmuth, W. D.; Austin, R. H. *Nature* **1992**, *358*, 600. (g) Ashton, R.; Padala, C.; Kane, R. S. *Curr. Opin. Biotechnol*. **2003**, *14*, 497. (h) Olson, D. J.; Johnson, J. M.; Patel, P. D.; Shaqfeh, E. S. G.; Boxer, S. G.; Fuller, G. G. *Langmuir* **2001**, *17*, 7396.

(4) (a) Rädler, J.; Strey, H.; Sackmann, E. *Langmuir* **1995**, *11*, 4539. (b) Nissen, J.; Gritsch, S.; Wiegand, G.; Rädler, J. O. *Eur. Phys. J. B* **1999**, *10*, 335. (c) Nissen, J.; Jacobs, K.; Rädler, J. O. *Phys. Rev. Lett.* **2001**, *86*, 1904. (d) Cremer, P. S.; Boxer, S. G. *J. Phys. Chem. B* **1999**, *103*, 2554. (e) Baumgart, T.; Offenhäusser, A. *Langmuir* **2002**, *18*, 5899. (f) Suzuki, K.; Masuhara, H. *Langmuir* **2005**, *21*, 537. (g) Suzuki, K.; Masuhara, H. *Langmuir*, **2005**, *21*, 6487.

(5) (a) Hulteen, J. C.; van Duyne, R. P. *J. Vac. Sci. Technol., A* **1995**, *13*, 1553. (b) Haynes, C. L.; van Duyne, R. P. *J. Phys. Chem. B* **2001**, *105*, 5599.

(6) (a) Groves, J. T.; Ulman, N.; Boxer, S. G. *Science* **1997**, *275*, 651. (b) Groves, J. T.; Ulman, N.; Cremer, P. S.; Boxer, S. G. *Langmuir* **1998**, *14*, 3347.

(7) Main transition temperature of egg-PC is far below room temperature. See: Chapman, D.; Williams, R. M.; Ladbrooke, B. D. *Chem. Phys. Lipids* **1967**, *1*, 445.

JA0559597